


# A Mammalian Target of Rapamycin-Perilipin 3 (mTORC1-Plin3) Pathway is essential to Activate Lipophagy and Protects Against Hepatosteatosis

Marina Garcia-Macia <sup>1,4</sup>, Adrián Santos-Ledo,<sup>5</sup> Jack Leslie,<sup>1</sup> Hannah L. Paish,<sup>1</sup> Amy L. Collins,<sup>1</sup> Rebecca S. Scott,<sup>1,6</sup> Abigail Watson,<sup>6</sup> Rachel A. Burgoyne,<sup>1</sup> Steve White,<sup>7</sup> Jeremy French,<sup>7</sup> John Hammond,<sup>7</sup> Lee A. Borthwick,<sup>1</sup> Jelena Mann,<sup>1</sup> Juan P. Bolaños,<sup>2,4</sup> Viktor I. Korolchuk,<sup>8</sup> Fiona Oakley,<sup>1</sup> and Derek A. Mann<sup>1</sup>

**BACKGROUND AND AIMS:** NAFLD is the most common hepatic pathology in western countries and no treatment is currently available. NAFLD is characterized by the aberrant hepatocellular accumulation of fatty acids in the form of lipid droplets (LDs). Recently, it was shown that liver LD degradation occurs through a process termed lipophagy, a form of autophagy. However, the molecular mechanisms governing liver lipophagy are elusive. Here, we aimed to ascertain the key molecular players that regulate hepatic lipophagy and their importance in NAFLD.

**APPROACH AND RESULTS:** We analyzed the formation and degradation of LD *in vitro* (fibroblasts and primary mouse hepatocytes), *in vivo* and *ex vivo* (mouse and human liver slices) and focused on the role of the autophagy master regulator mammalian target of rapamycin complex (mTORC) 1 and the LD coating protein perilipin (Plin) 3 in these processes. We show that the autophagy machinery is recruited to the LD on hepatic overload of oleic acid in all experimental settings. This led to activation of lipophagy, a process that was abolished by Plin3 knockdown using RNA interference. Furthermore, Plin3 directly interacted with the autophagy proteins focal adhesion interaction protein 200 KDa and autophagy-related 16L, suggesting that

Plin3 functions as a docking protein or is involved in autophagosome formation to activate lipophagy. Finally, we show that mTORC1 phosphorylated Plin3 to promote LD degradation.

**CONCLUSIONS:** These results reveal that mTORC1 regulates liver lipophagy through a mechanism dependent on Plin3 phosphorylation. We propose that stimulating this pathway can enhance lipophagy in hepatocytes to help protect the liver from lipid-mediated toxicity, thus offering a therapeutic strategy in NAFLD. (HEPATOLOGY 2021;74:3441-3459).

Caloric excess and sedentary lifestyle have led to a global epidemic of obesity and metabolic syndrome, and in association with these conditions up to one third of the population develop NAFLD.<sup>(1)</sup> NAFLD is the most frequent liver pathology in western countries<sup>(1)</sup> and in some individuals may progress to advanced severe fibrosis, cirrhosis, and cancer.<sup>(1)</sup> At present there are no clinically effective pharmacological treatments to prevent or ameliorate NAFLD or its progression to chronic liver disease.

*Abbreviations:* AAV, adeno-associated virus; Abca1, ATP-binding cassette transporter A1; ATG, autophagy-related; CMA, chaperon-mediated autophagy; Fip200, focal adhesion interaction protein 200 KDa; GTPase, guanosine triphosphatase; HFD, high-fat diet; iNOS, inducible nitric oxide synthase; Lamp, lysosomal-associated membrane protein; LC3, microtubule-associated protein 1A/1B-light chain 3; LD, lipid droplet; NLR, nucleotide-binding domain leucine-rich repeat; mTOR, mammalian target of rapamycin; mTORC, mammalian target of rapamycin complex; NIH-3T3, National Institutes of Health Swiss mouse embryo fibroblast; OA, oleic acid; OCR, oxygen consumption rate; PCLS, precision-cut liver slice; Plin, perilipin; Rag, recombination activating gene; Rheb, Ras homolog enriched in brain; Rictor, Rapamycin-insensitive companion of mTOR; TIMP1, tissue inhibitor of metalloproteinase 1; TSC, tuberous sclerosis.

Received August 15, 2020; accepted June 13, 2021.

Additional Supporting Information may be found at [onlinelibrary.wiley.com/doi/10.1002/hep.32048/supinfo](https://onlinelibrary.wiley.com/doi/10.1002/hep.32048/supinfo).

Supported by C0120R3166, C0245R4032, and BH182173 from Newcastle University. M. G.-M. is a Sara Borrell Postdoctoral fellow (CD18/00203) from the Ministerio de Ciencia, Innovación y Universidades (Spain). J. P. B. is funded by the Agencia Estatal de Investigación, grants PID2019-105699RB-I00/AEI/10.13039/501100011033 and RED2018-102576-T, Instituto de Salud Carlos III (CB16/10/00282), Junta de Castilla y León (Escalera de Excelencia CLU-2017-03), Ayudas Equipos Investigación Biomedicina 2017 Fundación BBVA, and Fundación Ramón Areces. V. I. K. acknowledges support from Biotechnology and Biological Sciences Research Council (BB/M023389/1, BB/R008167/1, BB/

NAFLD is characteristically associated with the accumulation of intracellular lipid droplets (LDs) within hepatocytes which if unchecked results in lipotoxicity and liver damage.<sup>(2)</sup> LDs are dynamic metabolic stations,<sup>(3)</sup> formed by a core of neutral lipids surrounded by a phospholipid membrane and proteins which includes members of the lipid sequestering perilipin (Plin) family. Plins coat LDs and help to control their biogenesis, stabilization, and prevent their degradation.<sup>(4)</sup> Plin2 and Plin3 are both expressed in hepatocytes,<sup>(4)</sup> which gives them the potential to influence hepatic lipid metabolism and NAFLD.<sup>(3)</sup>

LD catabolism can be initiated downstream of two distinct stimuli: nutrient deprivation and acute LD overload. Both scenarios have in common an increase in autophagy activity.<sup>(5,6)</sup> Autophagy is the cellular clearing and recycling program that degrades unwanted cytoplasmic content within lysosomes.<sup>(6,7)</sup> To date, two mechanisms for LD degradation through autophagy have been described. One involves chaperone-mediated

autophagy (CMA) where the LD perilipin Plin2 and probably also Plin3 binds to the lysosome protein lysosomal-associated membrane protein (Lamp) 2a and mediates LD uncoating before autophagosome engulfment.<sup>(3,8)</sup> The other involves macroautophagy (hereafter autophagy) where LDs are engulfed in the cytoplasm and delivered to the lysosome through autophagosome-lysosome fusion. This latter type of autophagy is called lipophagy.<sup>(6)</sup> Selective autophagic degradation of cellular organelles is mediated by specific receptor proteins.<sup>(9)</sup> However, to our knowledge, specific receptors for lipophagy remain unknown. From the LD-resident proteins, small guanosine triphosphatases (GTPases) of the Ras-associated binding protein family may potentially assist with the recruitment of the autophagic machinery to the LD,<sup>(10)</sup> but Plins are the only proteins specific to LDs.<sup>(3)</sup> Efficient lipophagy requires phosphorylation and subsequent degradation of Plin2 and Plin3.<sup>(8)</sup> Interestingly, Plin3 is found in CMA-deficient lysosomes in the fed state which indicates a distinct

R506345/1). R. S. S. is funded by the EU European Union regional development fund and FibroFind Ltd. A. L. C. is funded by the William E. Harker Foundation. D. A. M., J. M., L. A. B., and F. O. are funded by the Medical Research Council Programme Grants MR/K0019494/1 and MR/R023026/1. A CRUK Programme grant, reference C18342/A23390, supports J. L. and D. A. M.

© 2021 The Authors. HEPATOLOGY published by Wiley Periodicals LLC on behalf of American Association for the Study of Liver Diseases This is an open access article under the terms of the Creative Commons Attribution License, which permits use, distribution and reproduction in any medium, provided the original work is properly cited.

View this article online at [wileyonlinelibrary.com](http://wileyonlinelibrary.com).

DOI 10.1002/hep.32048

Potential conflict of interest: Dr. Borthwick received grants from GlaxoSmithKline, Nuformix, and Pfizer. He owns stock in FibroFind Ltd, FibroFind IP Ltd and FF Estates Ltd. Dr. J Mann received grants from GlaxoSmithKline and owns stock in FibroFind Ltd, FibroFind IP Ltd and FF Estates Ltd. Dr. Oakley received grants from GlaxoSmithKline and owns stock in FibroFind Ltd, FibroFind IP Ltd and FF Estates Ltd. Dr. DA Mann advises Andera Partners, received grants from GlaxoSmithKline, and owns stock in FibroFind Ltd, FibroFind IP Ltd and FF Estates Ltd. Dr. Leslie and H Paish own shares in FibroFind Ltd.

## ARTICLE INFORMATION:

From the <sup>1</sup>Newcastle Fibrosis Research Group, Biosciences Institute, Newcastle University, Newcastle upon Tyne, United Kingdom; <sup>2</sup>Institute of Biomedical Research of Salamanca, University Hospital of Salamanca, Salamanca, Spain; <sup>3</sup>Institute of Functional Biology and Genomics, University of Salamanca, CSIC, Salamanca, Spain; <sup>4</sup>Centro de Investigación Biomédica en Red sobre Fragilidad y Envejecimiento Saludable (CIBERFES), Instituto de Salud Carlos III, Madrid, Spain; <sup>5</sup>E.U.E Dacio Crespo (Universidad de Valladolid), Palencia, Spain; <sup>6</sup>FibroFind Ltd, William Leech Building, Medical School, Newcastle University, Newcastle upon Tyne, United Kingdom; <sup>7</sup>Department of Hepatobiliary Surgery, Newcastle upon Tyne Hospitals NHS Foundation Trust, Newcastle upon Tyne, United Kingdom; <sup>8</sup>Biosciences Institute, Newcastle University, Newcastle upon Tyne, United Kingdom.

## ADDRESS CORRESPONDENCE AND REPRINT REQUESTS TO:

Marina García-Macia, Ph.D.  
Biosciences Institute, Newcastle University  
Framlington Place  
NE2 4HH Newcastle upon Tyne, United Kingdom  
E-mail: [marinagarciamacia@gmail.com](mailto:marinagarciamacia@gmail.com)  
Tel.: +349-232-94907  
or

Derek A. Mann, Ph.D.  
Newcastle Fibrosis Research Group, Biosciences Institute,  
Newcastle University  
Framlington Place  
NE2 4HH Newcastle upon Tyne, United Kingdom  
E-mail: [derek.mann@newcastle.ac.uk](mailto:derek.mann@newcastle.ac.uk)  
Tel.: +1-44(0)-191-208-3851

degradation pathway and function for Plin3 compared with Plin2 which is only found in CMA-proficient lysosomes.<sup>(3)</sup>

The key cellular sensor of nutrients is the mammalian target of rapamycin (mTOR).<sup>(11)</sup> mTOR is the catalytic subunit of two distinct complexes, called mTOR complex (mTORC) 1 and mTORC2. These two complexes have unique protein components and respond to different cellular signaling events with distinct outcomes.<sup>(11)</sup> In nutrient replete conditions mTORC1 promotes cellular anabolism whilst suppressing autophagy. mTORC1 also promotes formation of LDs.<sup>(12)</sup> Interestingly, simultaneously with mTOR activation, high levels of nutrients including lipids serve to activate lipophagy and to prevent hepatic lipotoxicity.<sup>(6)</sup> The exact mechanisms behind these seemingly contradictory observations remain unresolved. To address this latter issue, we have emulated acute lipid overload with oleic acid (OA) treatment and high-fat diet (HFD feeding) in different experimental models (*in vitro*, *ex vivo*, and *in vivo*) and analyzed mechanisms allowing for simultaneous activation of mTOR and lipophagy.

Here, we identify phosphorylated Plin3 as a protein required for lipophagy after acute lipid overload, and mTOR as the kinase responsible for this phosphorylation. Our findings provide an important insight into the mechanisms of energy utilization in the liver and identify potential targets for the selective degradation of LDs which may lead to future therapeutic interventions in NAFLD.

## Materials and Methods

### MICE

Mice were housed in pathogen-free conditions and kept under standard conditions with a 12-hour day/night cycle and access to food and water *ad libitum*.

Male C57BL/6 mice were used for hepatocyte isolation (n = 5) and precision-cut liver slices (PCLS), generated from Plin3 knockdown mouse livers (n = 3 per experimental condition). Adenoviral mediated shRNA delivery was used to target the epithelial cells of the liver. C57BL/6 mice received a single intravenous tail vein injection of  $1 \times 10^{11}$  genome copies of adeno-associated virus (AAV) 8-GFP-U6-m-M6PRBP1-shRNA to knockdown Plin3 levels. Control mice received an equal dose of

AAV8-GFP-U6-m-null-shRNA. Animal experiments were approved by the Newcastle Ethical Review Committee and performed under a UK Home Office license in accordance with the Animal Research: Reporting of *In Vivo* Experiments guidelines.

*In vivo* experiments: male C57BL/6 mice (n = 5 per experimental condition) were fed with regular chow (Teklad global, Envigo, Indianapolis, IN) or HFD (D12451, Brogaarden Korn & Foderstoff, Denmark) for 4 weeks. Mice were subjected to an overnight starvation before harvesting. Animal procedures we performed according to the European Union Directive 86/609/EEC and Recommendation 2007/526/EC, regarding the protection of animals used for experimental and other scientific purposes, enforced in Spanish legislation under the directive RD1201/2005. All protocols were approved by the Bioethics Committee of the University of Salamanca.

### ISOLATION OF LD FRACTIONS

For the isolation of LDs from cultured cells, a modified method of Brasaemle<sup>(13)</sup> was used. Cells were homogenized in LD buffer (20mM Tris/Cl at pH 7.4 and 1mM EDTA with phosphatase and protease inhibitors) and centrifuged at 1,000× g for 10 minutes at 4°C. Supernatants were mixed with OptiPrep to obtain a suspension of 30%, which was placed in ultracentrifugation tubes (SW40 tubes; Beckman Coulter GmbH, Germany). This bottom layer was overlaid with 20% and 10% OptiPrep mixtures in LD buffer and finally with LD buffer supplemented with phosphatase and protease inhibitors. The gradients were centrifuged for 3 hours at 4°C and 40,000 rpm (SW40TI rotor). LD layers on top of the gradient were collected. This fraction was delipidated using methanol washes and solubilized in 2% SDS for immunoblotting.

LD fraction from mouse liver was isolated as described.<sup>(6)</sup> Glyceraldehyde 3-phosphate dehydrogenase was used to exclude cytosolic contamination and ponceau was used as a loading control.<sup>(14)</sup>

### HUMAN LIVER TISSUE

Normal control human liver tissue was collected from patients undergoing surgical resections and obtained under full ethical approval (H10/H0906/41

and CEPA biobank 17/NE/0070) and used subject to patients' written consent. No donor organs were obtain for executed prisoners or other institutionalized persons.

## PRECISION CUT SLICES

Mouse and human liver tissue slices were processed and maintained as described.<sup>(15)</sup>

## DRUG TREATMENTS

Cells were treated for 6 hours with 0.25 mM OA to induce the formation of LDs.<sup>(14)</sup>

To measure the effect of mTORC1 inhibition on lipophagy, cells were pretreated with rapamycin (20  $\mu$ M) before OA treatment for 1 hour. HFD fed mice were injected with rapamycin (4 mg/kg) IP before overnight starvation, some mice receive lysosomal inhibitors 2 hours before harvest.

To test mitochondrial use of lipids, cells were pretreated for 12 hours with Etomoxir (carnitine palmitoyltransferase 1a inhibitor, 100  $\mu$ M).

## AUTOPHAGIC MEASUREMENTS

We measured autophagy flux to quantify autophagy activity as described.<sup>(14)</sup> Briefly, accumulation of autophagy substrates, microtubule-associated protein 1A/1B-light chain 3 (LC3)-II or p62, or other substrates, e.g., Plin3, in the presence of inhibitors of lysosomal proteolysis (ammonium chloride [20mM] and leupeptin [100 $\mu$ M]) reflects autophagy activity. Cells were cultured with or without lysosomal inhibitors for 2 hours (4 hours after OA treatment) following which, cells were collected, lysed and subjected to immunoblotting for LC3-II or p62. Autophagy flux was calculated by subtracting the densitometric value of inhibitor-untreated LC3-II or p62 from the corresponding inhibitor-treated values.

## BIOENERGETICS

Oxygen consumption rates of National Institutes of Health Swiss mouse embryo fibroblast (NIH-3T3) cells and hepatocytes were measured in real-time in an XF96 Extracellular Flux Analyzer (Seahorse Bioscience, Billerica, MA). Details are described in the Supporting Information.

## STATISTICAL ANALYSIS

Data are represented as mean  $\pm$  SEM and are from a minimum of three independent experiments unless otherwise stated. Graphpad prism was used to perform ANOVA with a Tukey's post hoc test. \* $P$  < 0.05, \*\* $P$  < 0.01, or \*\*\* $P$  < 0.001 and # $P$  < 0.05, ## $P$  < 0.01, and ### $P$  < 0.001 was considered statistically significant.

## Results

### OA TREATMENT INDUCES LIPOPHAGY AND SELECTIVE DEGRADATION OF PLIN3

Cells treated with fatty acids emulate the lipid overload characteristic of the postprandial state and can be used to simulate disease conditions synonymous with those found in NAFLD.<sup>(16,17)</sup> OA treatment was chosen as it induces LD formation.<sup>(18,19)</sup> Autophagy is also triggered following OA treatment,<sup>(5)</sup> as OA increased LC3 flux (Supporting Fig. S1A). First, we asked if OA-triggered autophagy promoted selective degradation of LDs. NIH-3T3 fibroblasts or primary hepatocytes were cultured with OA and treated with or without lysosomal inhibitors before determination of autophagy flux. Autophagic flux (the dynamic process of autophagy) is monitored by western blot analysis of components of the autophagic machinery in the presence and absence of lysosomal degradation inhibitors. The difference in the levels of autophagy proteins LC3-II or p62 between the two conditions is directly proportionate to the flux through the autophagy pathway.<sup>(20)</sup> Western blot and immunofluorescence colocalization were therefore used as complementary approaches to analyze autophagic events in LDs (or "lipophagy" Fig. 1A). Proteins involved in autophagy initiation (focal adhesion interaction protein 200 KDa [Fip200], autophagy-related [Atg] 16L, and Beclin1) were detected in LDs after OA treatment and were increased after blocking lysosomal fusion (Fig. 1B). LC3-II and Lamp1 accumulated in LDs further indicating induction of lipophagy in response to OA (Fig. 1B). Plin3 was barely detectable in LDs but became abundant after lysosomal inhibition, this suggesting Plin3 is a preferential target for lysosomal degradation when compared with Plin2 which was readily detected in LDs in both the presence and

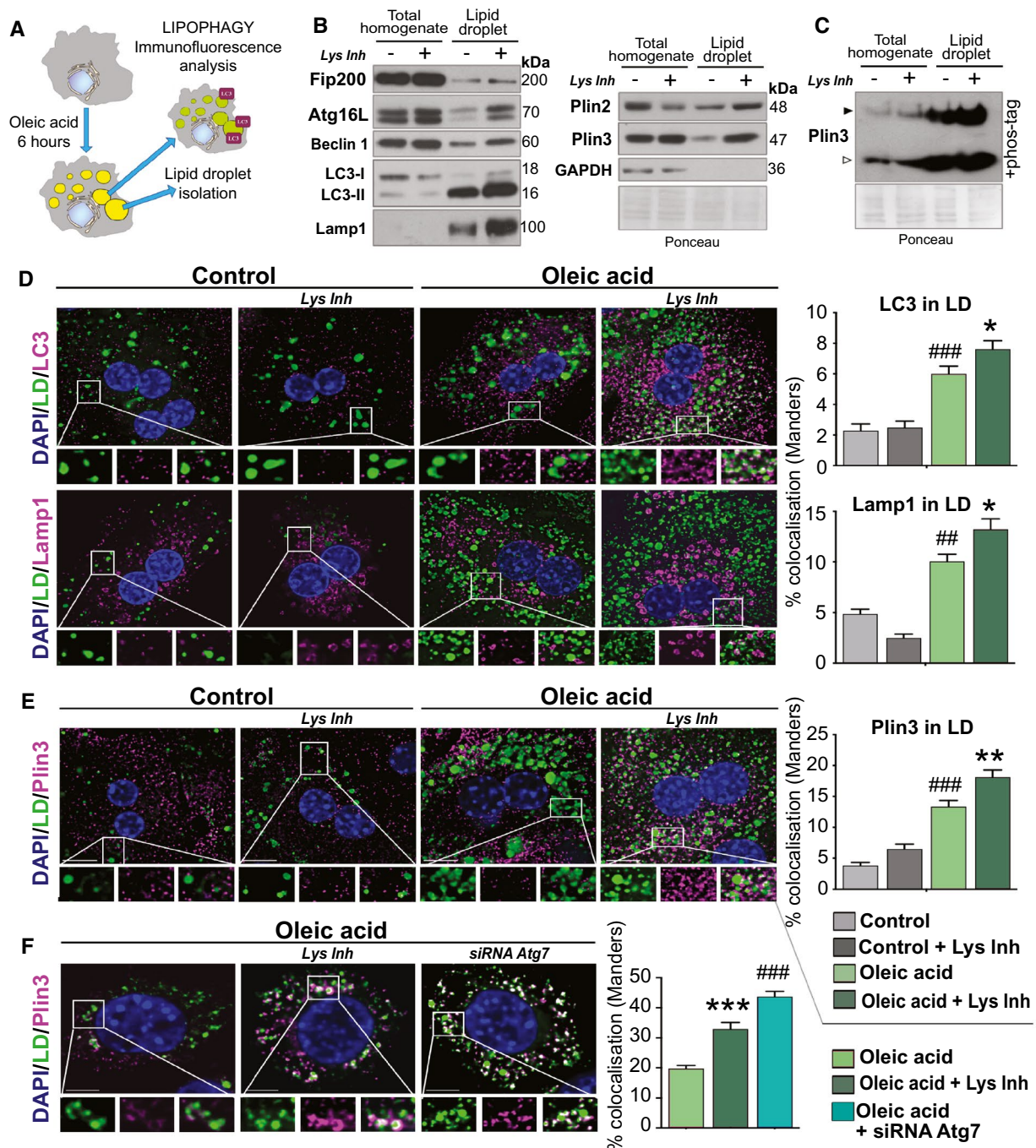


**FIG. 1.** OA treatment induces lipophagy and selective degradation of Plin3. (A) Depiction of the methodological approach: 0.25 mM OA treatment induces LD formation in primary hepatocytes and NIH-3T3 cells. Lipophagy is analyzed by immunofluorescence and western blotting in homogenates and isolated LDs. (B) Autophagy pathway proteins and Plins expression in total homogenates and LD isolations from NIH-3T3 cells after 6 hours of OA treatment with or without lysosomal inhibitors (Lys inh: 20 mM ammonium chloride and 100  $\mu$ M leupeptin) to test autophagy flux. (C) Total homogenates and LDs from NIH-3T3 cells were subjected to Phos-tag gel electrophoresis and immunoblotted for Plin3. Black arrowhead: P-Plin3; white arrowhead: Plin3. (D) LC3 and Lamp1 (magenta) recruitment to LDs (green) in the OA-treated primary hepatocytes (quantified in the histograms). (E) Plin3 (magenta) recruitment to LDs (green) (quantified in the histogram). (F) Plin3 recruitment to LDs in OA-treated NIH-3T3 cells and after blocking autophagy using Atg7 knockdown. Scale bar: 20  $\mu$ m. Data are mean  $\pm$  SEM. \* $P$  < 0.05, \*\* $P$  < 0.01, and \*\*\* $P$  < 0.001 (differences caused by lysosomal inhibitors treatment), ## $P$  < 0.01 and ### $P$  < 0.001 (differences caused by treatment). Fifty cells were analyzed from three experiments for each condition.

absence of lysosomal inhibitors (Fig. 1B and Supporting Fig. S1B). Plin3 degradation depends on its phosphorylation status, this enabling the autophagic machinery to access LDs.<sup>(3)</sup> Lysosome inhibition was associated with

an increase in the phosphorylated form of Plin3 (upper band) in LDs (Fig. 1C).

We next co-stained hepatocytes with LC3 and Lamp1 antibodies (Fig. 1D) together with 4,4-difl

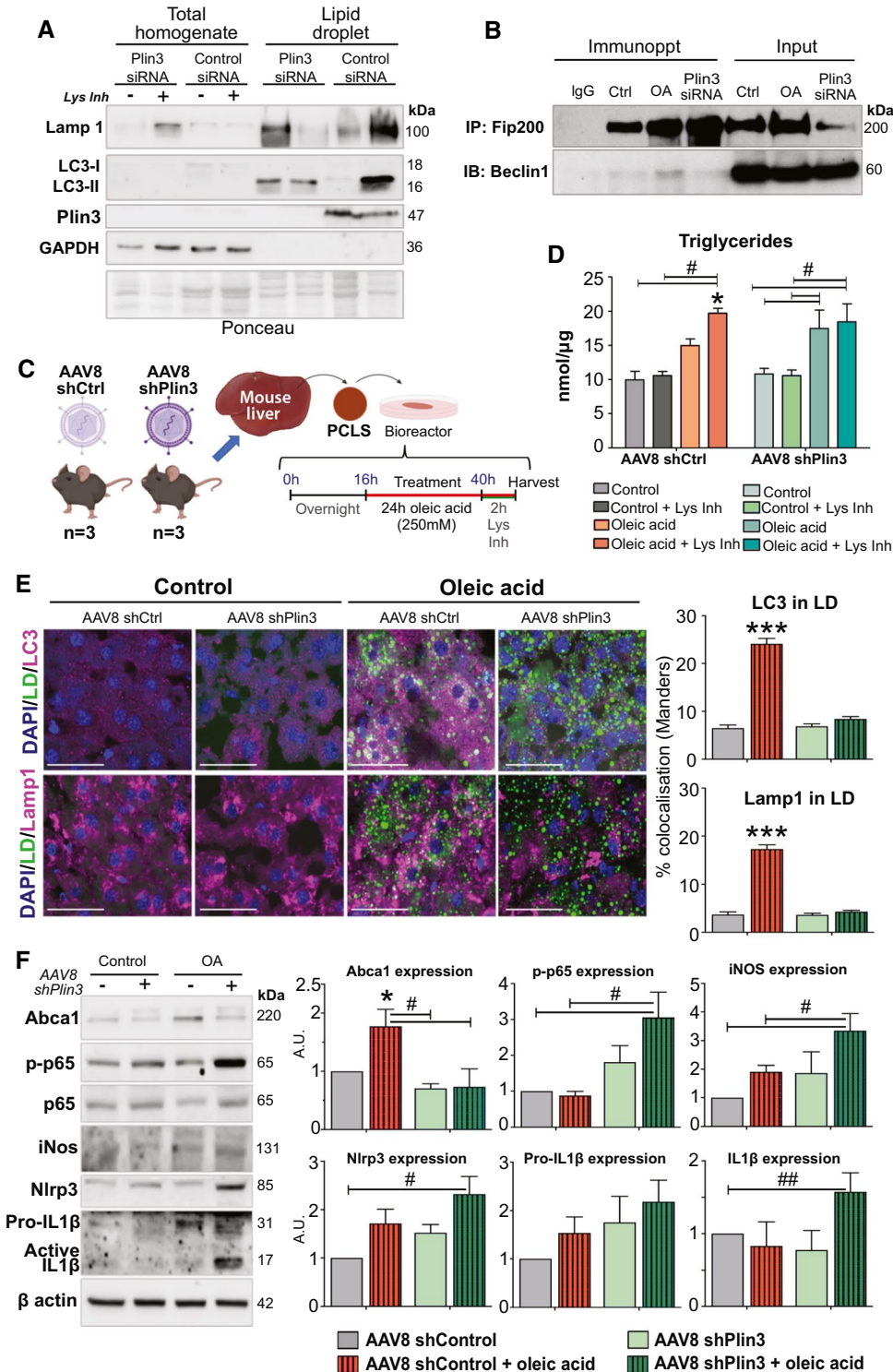


**FIG. 2.** Plin3 docks autophagy machinery to LDs. (A) Autophagy pathway proteins and Plin3 expression in total homogenates and LD isolations from NIH-3T3 cells silenced with Plin3 small interfering RNA (siRNA) or Scramble (control [Ctrl]) siRNA after 6 hours of 0.25 mM OA treatment with or without lysosomal inhibitors (Lys inh: 20 mM ammonium chloride and 100  $\mu$ M leupeptin) to test autophagy/lipophagy flux. (B) Immunoprecipitation of Fip200 in NIH-3T3 cells without and with OA treatment and Plin3 silenced cells treated with OA showing binding between Fip200 and Beclin1. (C) Depiction of the methodological approach: liver slices from AAV8-shCtrl or AAV8-shPlin3 mice are treated with or without 0.25 mM OA for 24 hours, then slices were treated with or without Lys inh (20 mM ammonium chloride and 100  $\mu$ M leupeptin) for 2 hours. (D) Triglyceride levels, expressed in nanomoles/micrograms of protein, in the Plin3 knockdown and control liver slices treated without or with 0.25 mM OA and treated without or with lysosomal inhibitors. (E) Recruitment of LC3 or Lamp1 (magenta) to LDs (green) in the Plin3 knockdown and control liver slices treated without or with OA (quantified in the histograms). (F) Levels of Abca1 and inflammatory proteins in total homogenates from Plin3 knockdown and control liver slices treated without or with OA (densitometry in the histograms). Scale bar: 50  $\mu$ m. Bars are mean  $\pm$  SEM. \* $P$  < 0.05 and \*\*\* $P$  < 0.001 (differences caused by lysosomal inhibitors treatment), # $P$  < 0.05, ## $P$  < 0.01, and ### $P$  < 0.001 (differences caused by treatment). Fifty cells were analyzed from three experiments for each condition.

uoro-4-bora-3a,4a-diaza-s-indacene (BODIPY), a dye for neutral lipids in LDs. Colocalization of LC3 and Lamp1 with LDs was increased in OA-treated hepatocytes (Fig. 1D;  $P$  < 0.01) and a further modest increase was seen on exposure to lysosomal inhibitors (Fig. 1D;  $P$  < 0.001). A similar pattern was observed for Plin3 colocalization with LDs (Fig. 1E;  $P$  < 0.01) and lysosomal marker Lamp1 (Supporting Fig. S1C;  $P$  < 0.001). Knockdown of an essential autophagy protein Atg7 (Supporting Fig. S1D) also enhanced Plin3 accumulation at the LD surface of OA-treated NIH-3T3 cells (Fig. 1F;  $P$  < 0.001) supporting the concept of Plin3 as a selective cargo for OA-induced lipophagy. Based on these data, we conclude that lipid overload induces lipophagy and the selective degradation of Plin3.

## PLIN3 MAY PROMOTE RECRUITMENT OF AUTOPHAGY MACHINERY TO LDS

Targeted knockdown of Plin3 had no effect on expression of the autophagy core machinery (Supporting Fig. S2A). However, autophagic flux of LD-associated LC3-II and Lamp1 was disrupted in Plin3 silenced NIH-3T3 cells (Fig. 2A). Treatment of cells with OA and lysosomal inhibitors increased the colocalization of LC3 and Lamp1 with the LDs (Supporting Fig. S2B). Recruitment of these proteins to LDs was strongly suppressed in Plin3 silenced cells (Supporting Fig. 2B;  $P$  < 0.01). Triglycerides increased after OA treatment but to a greater extent in Plin3 knockdown cells compared with controls. However, when control cells were treated with lysosomal inhibitors, triglycerides were elevated to levels comparable with those of Plin3 knockdown cells (Supporting

Fig. S2C;  $P$  < 0.01). Hence, Plin3 is required for lipophagy and the control of triglyceride turnover in response to lipid loading.

To further confirm Plin3 as a component of the LD autophagy machinery, we probed for Fip200 and Atg16L in the immunoprecipitated endogenous Plin3 fractions. The association of these proteins with Plin3 increased following OA treatment (Supporting Fig. S2D), this being suggestive of Plin3 physically associating with the autophagy machinery in response to lipid loading. Treatment with the mTOR inhibitor rapamycin suppressed these interactions. These data were confirmed *in vivo* using liver homogenates from mice fed regular chow or HFD. Immunoprecipitation experiments showed that Plin3 interacts with mTOR as well as Fip200 and Atg16L (Supporting Fig. S2E). Immunofluorescence analysis of mTOR and Plin3 revealed that these proteins also colocalize in a manner that is accentuated by treatment with OA and lysosomal inhibitors (Supporting Fig. S3A). Fip200 is recruited to the sites of autophagosome biogenesis, preceding and facilitating the recruitment of other Atg proteins such as Beclin1.<sup>(21)</sup> We were thus interested to determine if Plin3 influences these interactions. To this end, endogenous Fip200 pull-downs were examined using cells cultured with or without OA treatment and Plin3 silencing. The interaction of Fip200 and Beclin1 was increased after OA treatment; however, the interaction was suppressed in Plin3 silenced NIH-3T3 cells (Fig. 2B). Recruitment of the lipases ATGL and HSL to LDs were similar between control and Plin3 silenced cells confirming that the classical lipolysis pathways remained intact (Supporting Fig. S3B,C). These results indicate a crucial role for Plin3 either in the recruitment of autophagic machinery to LDs or in the formation of the autophagosome in the LD.

We next asked if Plin3 is involved in control of the inflammatory response to lipid challenge. To this end, PCLS were generated from mice in which hepatocyte-selective depletion of Plin3 was achieved using an AAV8-shPlin3 (Fig. 2C). Successful knockdown of Plin3 was confirmed by immunofluorescence and western blotting (Supporting Fig. S3D). OA increased triglycerides levels in PCLS but to a greater extent when Plin3 expression was suppressed (Fig. 2D;  $P < 0.05$ ). Lysosomal inhibition of OA-treated control-AAV PCLS enhanced triglycerides to levels seen in Plin3 deficient PCLS treated with OA (Fig. 2D). Hence, suppressing Plin3 or blocking autophagy has a similar impact on lipid turnover supporting a role for Plin3 as a lipophagy regulator. As anticipated, LC3 or Lamp1 (magenta) recruitment to LD (green) was increased in control PCLS exposed to OA, but not in Plin3 knockdown PCLS (Fig. 2E;  $P < 0.001$ ). Loss of Plin3 had no effect on expression of the hepatic macroautophagy core machinery or tissue function (Supporting Fig. S3E,F). The ATP-binding cassette transporter A1 (Abca1) mediates the rate-limiting step of HDL biogenesis and suppresses inflammation.<sup>(22)</sup> Abca1 expression was induced in OA-treated PCLS in a Plin3-dependent manner (Fig. 2F;  $P < 0.05$ ). This indicates defective lipid handling in Plin3 deficient hepatocytes, which in turn may promote inflammation. Phospho-p65 (p-p65), a marker of active NF- $\kappa$ B signaling, increased in OA-treated PCLS generated from Plin3 knockdown mice when compared with controls (Fig. 2F;  $P < 0.05$ ). Elevated expression of p-p65 was accompanied by increases in the proinflammatory mediators inducible nitric oxide synthase (iNos), nucleotide-binding domain leucine-rich repeat, nucleotide-binding domain and leucine-rich repeat containing family pyrin domain containing 3 (Nlrp3), and IL-1 $\beta$  (Fig. 2F;  $P < 0.01$ ). We conclude that hepatocellular Plin3 is required to maintain lipid processing and liver homeostasis in the fed state.

## MTORC1 ASSOCIATES WITH LDS

Overfeeding and lipid overload activate mTORC1, as confirmed by phosphorylation of S6 (Supporting Fig. S4A).<sup>(23)</sup> Total and phosphorylated mTOR (Ser2448) were increased in LDS on blockade of lysosomal activity (Fig. 3A). Regulatory-associated protein of mTOR subunit of mTORC1 slightly increased in LDS after treatment with lysosomal inhibitors, whereas mTORC2

component Rictor was unchanged (Fig. 3A). Similarly, Ras homolog enriched in brain (Rheb), the master activator of mTORC1 was increased in LDS of lysosomal inhibitor-treated cells (Fig. 3A). Activation of mTORC1 requires its recruitment to the surface of the lysosome mediated by recombination activating gene (Rag) GTPases, Rag A/B or Rag C/D.<sup>(24)</sup> These proteins were also found in LD fractions, thus accounting for all the key components of mTORC1 complex, moreover RagA and RagB accumulated in LDS on blockade of lysosomal function, this suggesting they may be degraded during lipophagy (Fig. 3A). Of note, tuberous sclerosis (TSC) 1, an mTOR inhibitor, was absent in LDS. These data support the presence of the machinery required for mTORC1 activation in LDS and reveals an unexpected subcellular localization for mTORC1.

In agreement with western blot data, mTOR colocalization with LDS in hepatocytes after OA treatment was further increased after blocking lysosomal function (Fig. 3B;  $P < 0.001$ ). mTOR was also accumulated in LDS of OA-treated NIH-3T3 cells following Atg7 knockdown and at a level equivalent to that observed on the treatment with lysosomal inhibitors (Fig. 3C;  $P < 0.05$ ). Together these data indicate that mTORC1 is present on LDS, potentially anchored to their surface by Rag GTPases. Active, phosphorylated mTOR is present on LDS consistently with the presence of its master activator Rheb. Interestingly, components of mTORC1 in LDS appear to undergo lysosomal degradation mediated by autophagy.

## ROLE OF PLIN3 IN LIPOPHAGY IS CONTROLLED BY MTORC1

We next asked if there is a functional relationship between mTORC1 and Plin3 in LDS of OA-treated cells by either inhibiting mTOR with rapamycin (hepatocytes) or silencing mTORC1 (NIH-3T3) (Fig. 4A). Suppression of mTOR was confirmed by inhibition of phosphorylation of its downstream target S6 kinase which in control cells was robustly induced by OA (Supporting Fig. S4A,B). p-mTOR was barely detectable in LDS after rapamycin treatment (Fig. 4B). Similarly, rapamycin decreased Rheb in LDS and suppressed OA-induced LD accumulation of Atg16L, Beclin 1 and Fip200 (Fig. 4B). LC3-II and Lamp1 recruitment to LDS was also inhibited by rapamycin (Fig. 4B). This disturbance of the autophagy machinery in LDS was corroborated



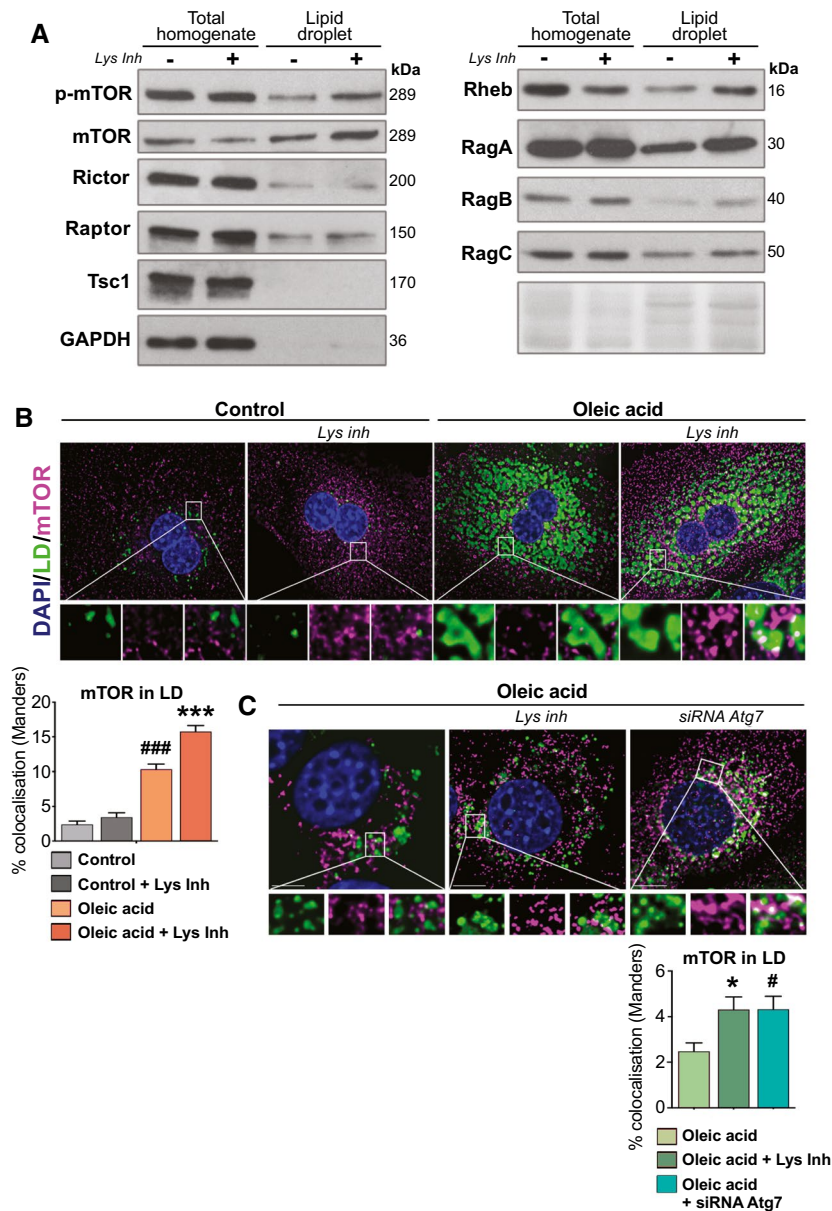


**FIG. 3.** mTORC1 machinery is present in LDs. (A) Levels of mTOR pathway proteins: phosphorylated mTOR (p-mTOR), mTOR, regulatory-associated protein of mTOR (Raptor), Rheb, RagA, B, and C, Rictor, and Tsc1 in total homogenates and LD isolations from NIH-3T3 cells at 6 hours of 0.25 mM OA treatment without and with lysosomal inhibitors (Lys inh: 20 mM ammonium chloride and 100  $\mu$ M leupeptin). (B) mTOR (magenta) recruitment to LDs (green) in the OA-treated primary hepatocytes without and with lysosomal inhibitors (quantified in the histogram). (C) mTOR recruitment in Atg7 silenced and OA-treated NIH-3T3 cells (quantified in the histogram). Scale bar: 20  $\mu$ m. Bars are mean  $\pm$  SEM. \* $P$  < 0.05 and \*\*\* $P$  < 0.001 (differences caused by lysosomal inhibitors treatment), # $P$  < 0.05 and ### $P$  < 0.001 (differences caused by treatment). Fifty cells analyzed from three experiments for each condition.

by colocalization analyses (Fig. 4C; Supporting Fig. S4C). From these data, we would expect overactivation of mTOR to enhance mobilization of the autophagic machinery to LDs, this was confirmed

in NIH-3T3 cells depleted of the mTOR inhibitor TSC1 which displayed elevated pS6 and increased accumulation of LC3 in LDs (Supporting Fig. S4D). Conversely, rapamycin treatment or mTOR silencing

enhanced Plin3 accumulation on LDs and blocked autophagic flux (Fig. 4C;  $P < 0.05$ ; Supporting Fig. S4C). Rapamycin also stimulated triglyceride

accumulation (Fig. 4D;  $P < 0.001$ ) indicating that disruption of mTOR abrogates the autophagic lipid flux induced by OA. We then determined

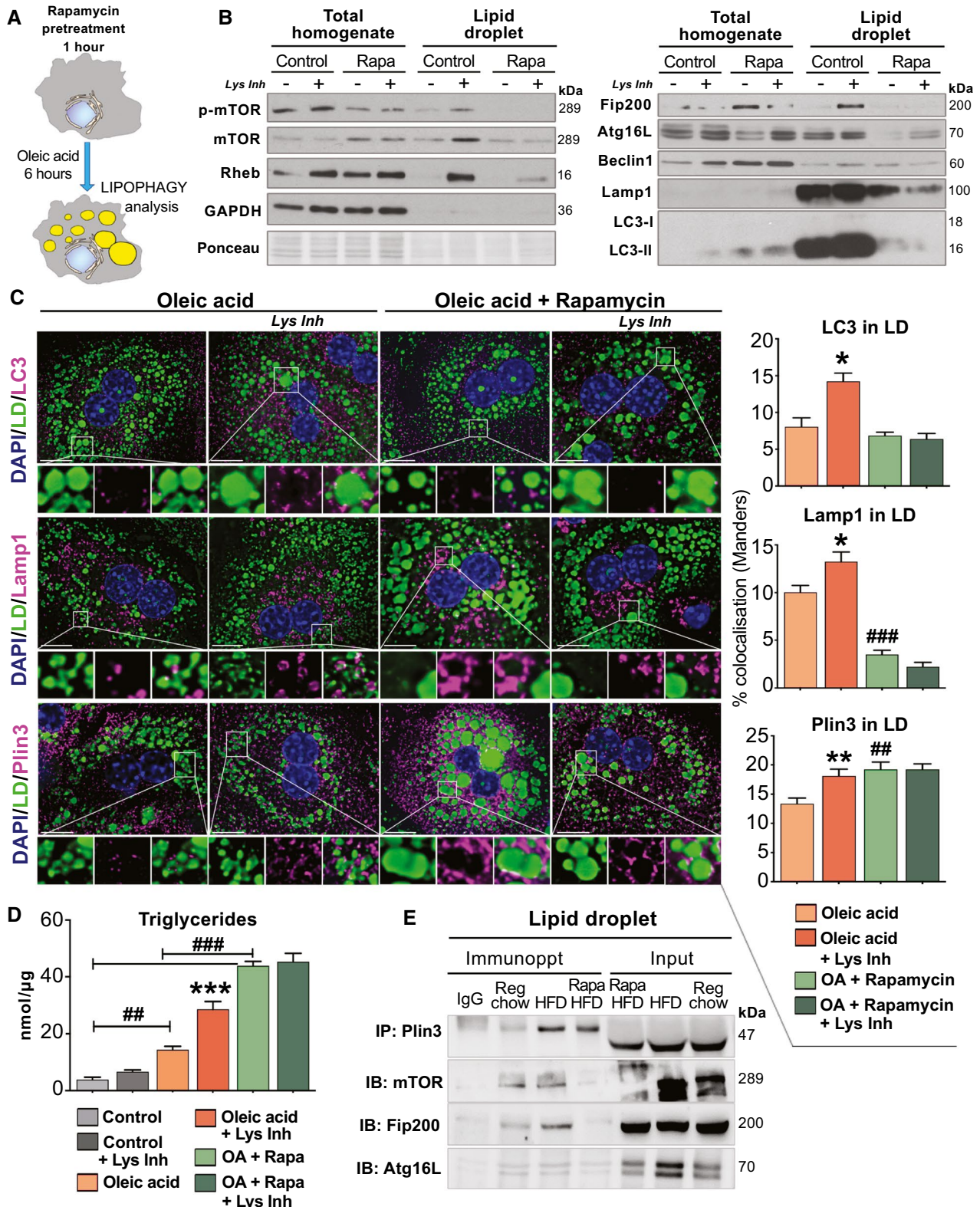


**FIG. 4.** The role of Plin3 on LDs is controlled by mTORC1 activity. (A) Depiction of the methodological approach: 20  $\mu$ M rapamycin was added 1 hour before the induction of LD formation by 0.25 mM OA treatment. Lipophagy is tested as previously described. (B) Autophagy and mTORC1 pathway protein levels in total homogenates and LD isolations from NIH-3T3 cell at 6 hours of OA treatment with and without 20  $\mu$ M rapamycin pretreatment. (C) LC3, Lamp1, and Plin3 (magenta) recruitment to LDs (green) in hepatocytes treated for 6 hours with OA without and with 20  $\mu$ M rapamycin pretreatment (quantified in the right column histograms). (D) Triglyceride levels in the hepatocytes pretreated or not with 20  $\mu$ M rapamycin, without or with 0.25 mM OA and treated without or with lysosomal inhibitors (Lys inh: 20 mM ammonium chloride and 100  $\mu$ M leupeptin), results are expressed in nanomoles/micrograms of protein. (E) Binding between Plin3 and the autophagy initiator proteins Fip200, Atg16L, and mTOR assessed by the coimmunoprecipitation with liver LDs endogenous Plin3 from regular chow, HFD, and rapamycin-treated HFD-fed mice. Scale bar: 20  $\mu$ m. Bars are mean  $\pm$  SEM. \* $P$  < 0.05, \*\* $P$  < 0.01, and \*\*\* $P$  < 0.001 (differences caused by lysosomal inhibitors treatment), ## $P$  < 0.01, and ### $P$  < 0.001 (differences caused by treatment). Fifty cells analyzed from three experiments for each condition.

involvement of mTORC1 in Plin3-mediated recruitment of autophagy machinery to LDs. Both Fip200 and Atg16L were co-precipitated with Plin3 on LDs formed in the liver of mice fed regular chow or HFD and these interactions were suppressed in rapamycin treated mice (Fig. 4E) and in isolated LDs from OA-treated cells (Supporting Fig. S4E). Finally, mTORC1 inhibition reduced the levels of phosphorylated Plin3 and the flux effect was abolished (Supporting Fig. S4F). We conclude that Plin3 phosphorylation by mTOR is a key event in docking the autophagic machinery to LDs during lipophagy.

### INHIBITION OF MTORC1-PLIN3 AXIS SUPPRESSES FUELING OF THE MITOCHONDRIA BY FATTY ACIDS

OA-treated primary hepatocytes displayed higher mitochondrial and maximal respiration than when cultured under basal conditions (Fig. 5A). As anticipated, this effect was suppressed by the fatty acid oxidation inhibitor etomoxir. Repression of respiration was also observed on treatment with lysosomal inhibitors or rapamycin, the later confirming that mTOR is required for lipophagy. Similar effects were observed in NIH-3T3 cells where we additionally tested the effects of knockdown of Plin3 (Fig. 5B). Relative to scramble control, Plin3-depleted cells failed to increase respiration in response to OA loading. To corroborate these findings, we also demonstrated repressive effects of lysosomal inhibitors, rapamycin and Plin3 knockdown on ATP production (Fig. 5C). Of note, cellular proliferation was not affected by the inhibitors or Plin3 knockdown (Supporting Fig. S5). We conclude that the mTOR-Plin3 axis is crucial for mobilization of fat for energy generation.

### RAPAMYCIN TREATMENT INDUCES INFLAMMATORY AND FIBROTIC FEATURES IN MICE ON HFD

To address the pathological implications of the mTORC1-Plin3 axis *in vivo*, we fed mice with regular chow or HFD for a month before an overnight fasting to induce a lipophagic response. Rapamycin was administered immediately before overnight starvation in the HFD group to suppress mTOR. Mice in each group were also treated either with or without lysosomal inhibitors at 2 hours before harvest (Supporting Fig. S6A). Efficacy of rapamycin in HFD fed mice was confirmed by a reduction in S6 phosphorylation and stimulation of autophagic flux (Supporting Fig. S6B,C). Consistent with *in vitro* observations, mTOR and the autophagic proteins Lamp1, ATG16L, Beclin1, and LC3 II were less abundant in LD isolated from the livers of HFD fed mice treated with rapamycin, and autophagic flux was abolished (Supporting Fig. S6D). Plin3 phosphorylation in the LD fraction was increased in the livers of chow and HFD fed mice after lysosomal inhibition but absent in rapamycin treated animals (Supporting Fig. S6E). HFD was associated with increased number and size of hepatic LDs compared with chow diet (Fig. 6A;  $P$  < 0.001, and Supporting Fig. S7A). Rapamycin treatment further increased LD size indicative of impaired lipid metabolism in the absence of mTOR activity. Lysosomal lipid flux quantified by the accumulation of triglycerides (TGs) on lysosomal blockade, is a physiological measure of the autophagic degradation of LDs. Regular chow and HFD mice showed a significant lipid flux when treated with lysosomal inhibitors, indicating active degradation of LDs through autophagy (Fig. 6B;  $P$  < 0.001). However, rapamycin prevented lipophagy and abrogated the

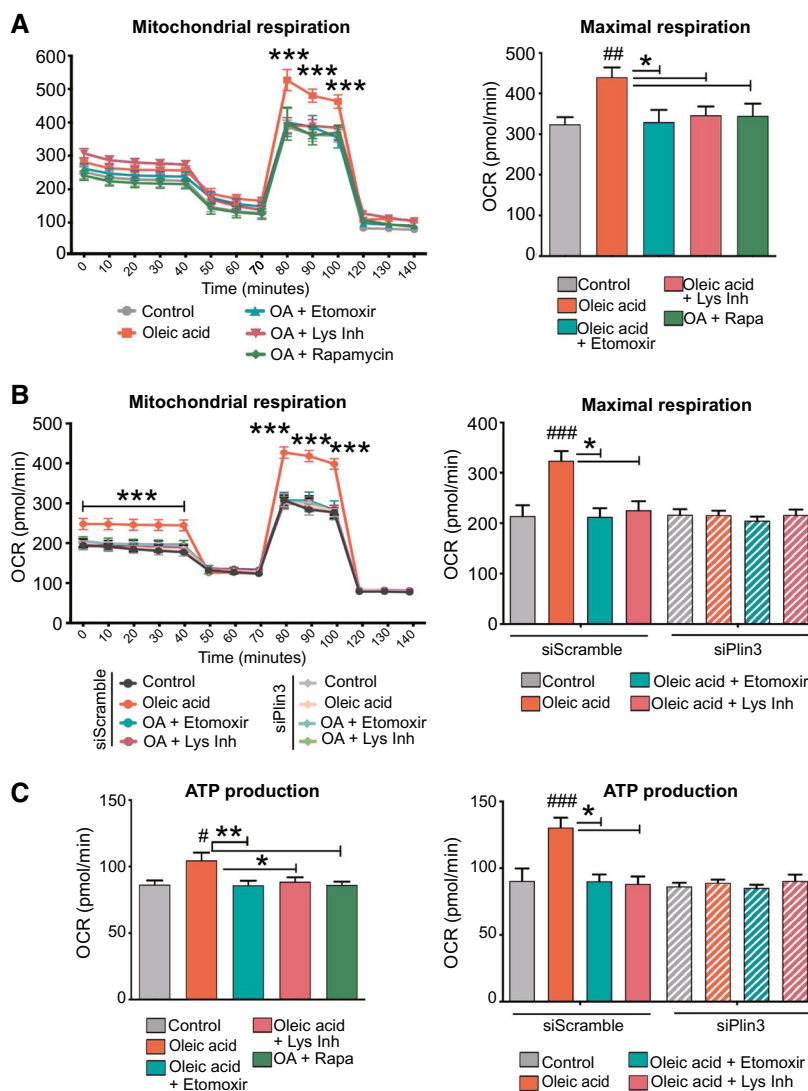


**FIG. 5.** Lipophagy produces fuel for mitochondria which is inhibited on mTORC1 inactivation. (A) Mitochondrial respiration and maximal respiration, expressed by oxygen consumption rate (picomole/minute), in primary hepatocytes under basal condition and after 6 hours of 0.25 mM OA treatment with and without etomoxir (100 nM), rapamycin pretreatment (20  $\mu$ M), or lysosomal inhibitors (Lys inh: 20 mM ammonium chloride and 100  $\mu$ M leupeptin). (B) Respiration of control and maximal respiration, expressed by oxygen consumption rate (picomole/minute), in small interfering scrambled RNA (siScramble) control or Plin3-silenced NIH-3T3 cells under basal condition and after 6 hours of 0.25 mM OA treatment with and without etomoxir (100 nM) or lysosomal inhibitors pretreatment. (C) ATP production in hepatocytes in response to OA treatment, with or without etomoxir, lysosomal inhibitors, or rapamycin (left graph) or in siScramble control NIH-3T3 or Plin3 silenced NIH-3T3 cell with or without 0.25 mM OA treatment with or without etomoxir (100 nM) or lysosomal inhibitors pretreatment. Bars are mean  $\pm$  SEM. \* $P$  < 0.05, \*\* $P$  < 0.01, and \*\*\* $P$  < 0.001 (differences caused by lysosomal inhibitors treatment), # $P$  < 0.05, ## $P$  < 0.01, and ### $P$  < 0.001 (differences caused by treatment).

flux leading to an accumulation of TGs (Fig. 6B;  $P$  < 0.01). Collectively, these data confirm that the mTORC1-Plin3 pathway is preserved *in vivo* and is required for hepatic lipid homeostasis.

Abca1 expression was suppressed in the rapamycin treated mouse livers (Fig. 6C;  $P$  < 0.05), indicative

of defective lipid handling which was reflected by a reduction in serum fatty acid levels (Supporting Fig. S7B;  $P$  < 0.001). To gain insight into the potential pathological implications for the mTORC1-Plin3 axis in our model, inflammatory mediators were quantified. Phospho-p65 (active canonical NF- $\kappa$ B pathway)

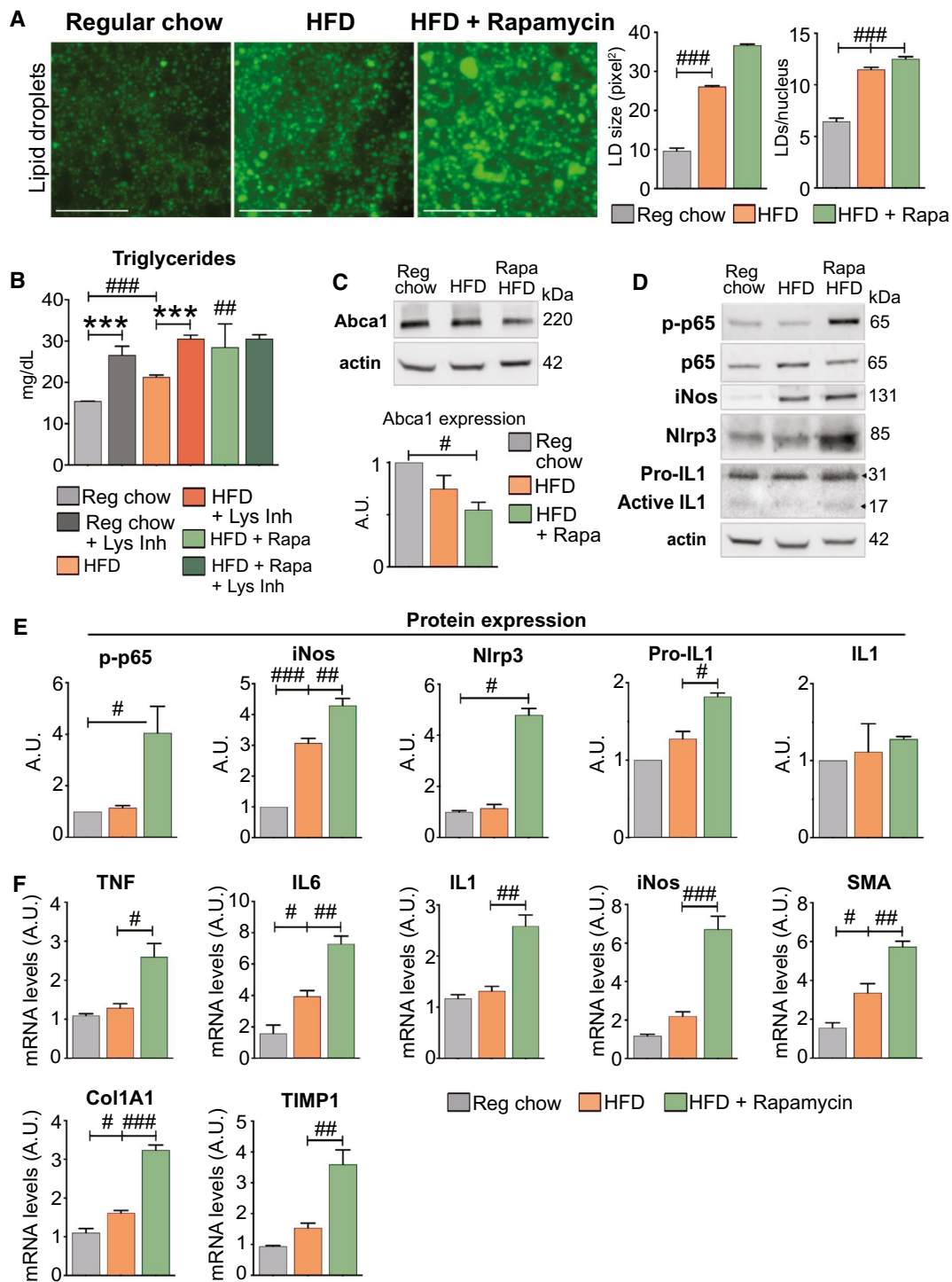


**FIG. 6.** Rapamycin treatment induces inflammatory and fibrotic features. (A) LDs size expressed as pixel<sup>2</sup> and LD numbers expressed as LDs/nucleus in liver slices from regular chow, HFD, and 4 mg/kg rapamycin-treated HFD-fed mice. (B) Liver triglycerides in regular chow, HFD, and rapamycin-treated HFD-fed mice expressed by milligrams/deciliters. (C) Levels of Abca1 and (D) inflammatory proteins expression in total homogenates from all conditions (quantified in the histograms). (E, F) Expression of the inflammatory genes (TNF $\alpha$ , IL-6, IL-1 $\beta$ , and iNos) and fibrogenic genes, TIMP1, alpha smooth muscle actin ( $\alpha$ SMA), and type IA1 collagen (Col1A1), expression from all conditions. Scale bar: 50  $\mu$ m. Bars are mean  $\pm$  SEM. \*\*\* $P$  < 0.001 (differences caused by lysosomal inhibitors treatment), # $P$  < 0.05, ## $P$  < 0.01, and ### $P$  < 0.001 (differences caused by treatment/diet) ( $n$  = 5 mice for each treatment).

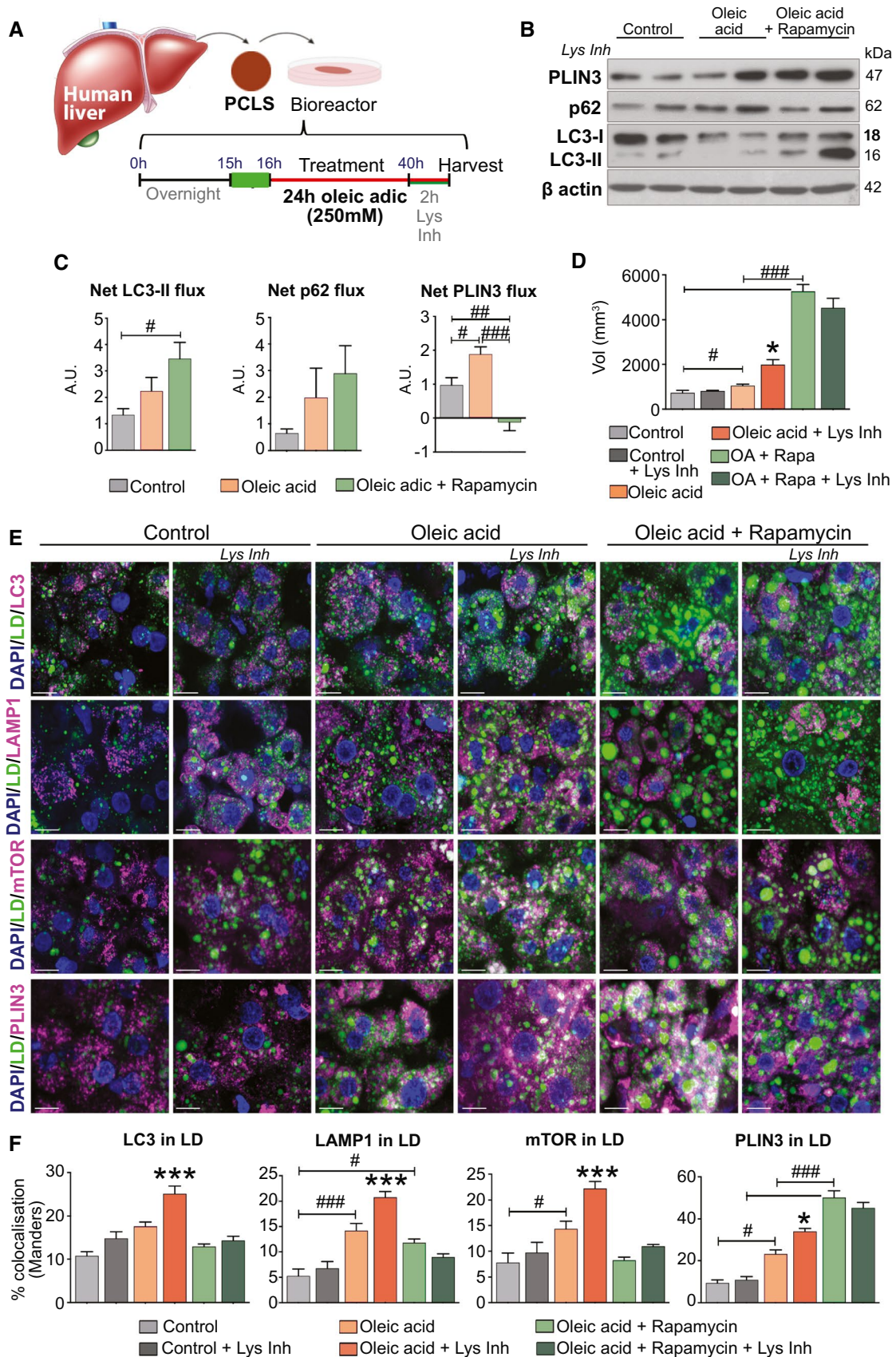


**FIG. 7.** Rapamycin treatment in human liver slices drives fat accumulation. (A) Depiction of the methodological approach: human liver slices are pretreated with or without 20  $\mu$ M rapamycin for 1 hour before the 0.25 mM OA treatment, and then slices are treated with or without lysosomal inhibitors (Lys inh: 20 mM ammonium chloride and 100  $\mu$ M leupeptin). (B, C) Levels of autophagy proteins and Plins in total homogenates from all the conditions. Black arrow LC3 II expression. Graphs show Net LC3-II, p62 and Plin3 flux. (D) Volume of LDs expressed as millimeters cubed (measure from LD staining in green) from all conditions. (E, F) Recruitment of LC3, Lamp1, or mTOR (magenta) to LDs (green) in the slices from all conditions (see E, quantified in F). Scale bar: 20  $\mu$ m. Bars are mean  $\pm$  SEM. \* $P < 0.05$  and \*\*\* $P < 0.001$  (differences caused by lysosomal inhibitors treatment), # $P < 0.05$ , ## $P < 0.01$ , and ### $P < 0.001$  (differences caused by treatment).

increased in the rapamycin treated livers compared with the regular chow-fed mice (Fig. 6D,E;  $P < 0.05$ ). NF- $\kappa$ B target genes: iNos, Nlrp3 and IL-1 $\beta$  showed the highest expression in the rapamycin treated mice. IL-1 $\beta$  increase was only significant for its precursor (pro-IL-1 $\beta$ ) (Fig. 6D,E;  $P < 0.05$ -0.001). To confirm the inflammatory response caused by rapamycin, we analyzed other markers such as tumor necrosis factor  $\alpha$  (TNF $\alpha$ ), IL-6, IL-1 $\beta$  and iNos through qRT-PCR. Only IL-6 was induced by HFD feeding, but expression of all inflammatory markers was increased when rapamycin was administered in combination with HFD (Fig. 6F;  $P < 0.05$ ). Persistent inflammation can drive fibrogenesis, which in turn promotes the net deposition and maturation of fibril-forming collagen-rich extracellular matrix, inducing liver fibrosis,<sup>(25)</sup> a common pathologic process associated with most chronic liver diseases including hepatic steatosis. Fibrogenic genes  $\alpha$ -smooth muscle actin, type IA1 collagen were elevated in HFD mice livers (Fig. 6F;  $P < 0.05$ ), as reported<sup>(26)</sup> and were further induced by rapamycin. Tissue inhibitor of metalloproteinase 1 (TIMP1) was not significantly increased in HFD mouse tissues but was induced on rapamycin treatment (Fig. 6F;  $P < 0.01$ -0.001). Finally, we measured serum aspartate aminotransferase (AST) levels (Supporting Fig. S7C), which were unaffected following one month of HFD diet; however, the combination of HFD and rapamycin treatment modestly increased AST levels (Supporting Fig. S7C;  $P < 0.05$ ). Therefore, both inflammatory and fibrogenic hallmarks increase on rapamycin treatment in the context of an HFD which underlies the relevance of the Plin3-mTORC1 axis to prevent lipid-mediated liver pathology.

## MTORC1 INHIBITION IN HUMAN LIVER SLICES DRIVES FAT ACCUMULATION

Excised human liver tissues were processed to generate PCLS cultures in which the role of the

mTORC1-Plin3 pathway could be determined in the context of intact human liver tissue<sup>(27)</sup> Liver slices were exposed to all previously stated treatments (Fig. 7A). Tissue function, as determined by albumin production, was not significantly affected by addition of OA, rapamycin or lysosomal inhibition (Supporting Fig. S8A). The efficacy of rapamycin on PCLS was confirmed by a reduction in S6 phosphorylation (Supporting Fig. S8B). OA treatment increased autophagy activity along with enhanced LC3, p62 and PLIN3 flux (Fig. 7B,C;  $P < 0.05$ ). Whilst the LC3 and p62 flux was increased by rapamycin, PLIN3 flux was suppressed, indicative of defective lipophagy (Fig. 7B,C;  $P < 0.001$ ). The volume of LDs was analyzed by the quantification of BODIPY and data confirmed that OA treatment increased LD volume (Fig. 7D;  $P < 0.05$ ). Consistent with the block of PLIN3 degradation by rapamycin, mTORC1 inhibition also stimulated an accumulation of LDs (Fig. 7D;  $P < 0.001$ ). Furthermore, IL-8 and TIMP1 proteins were detected in the media of PCLS at significantly increased levels after rapamycin treatment indicative of a proinflammatory and pro-fibrogenic state (Supporting Fig. S8C,D;  $P < 0.001$ ). Colocalization of LC3, LAMP1 and of mTOR with LDs, as measured by immunofluorescence, increased in hepatocytes following OA treatment (Fig. 7E,F;  $P < 0.001$ ,  $P < 0.05$ , respectively), and this was further increased when lysosomal activity was blocked. The colocalization of LC3 and LAMP1 with LDs was prevented by rapamycin (Fig. 7E,F;  $P < 0.05$ ), this confirming inhibition of lipophagy. Similarly, recruitment of PLIN3 to LDs was enhanced following OA treatment and further increased by lysosomal inhibitors (Fig. 7E,F;  $P < 0.05$ ). Akin to our cell culture and *in vivo* studies, rapamycin treatment promoted a strong accumulation of PLIN3 on LDs (Fig. 7F;  $P < 0.001$ ), supporting our hypothesis that mTORC1-PLIN3 axis plays a key role in the process of lipophagy in human liver.

## Discussion

Several groups have attempted to modulate mTORC1 signaling as a treatment for insulin resistance in obesity. However, mTORC1 inhibitors, such as rapamycin, produce adverse side effects including hyperlipidaemia and activation of gluconeogenesis in the liver.<sup>(28)</sup> Furthermore, around 55% of patients with posttransplant livers treated with rapamycin also develop hyperlipidaemia and have an increased risk of cardiovascular disease.<sup>(29)</sup> The reasons for these clinical side effects are largely unknown. mTORC1 is implicated in lipogenesis<sup>(30)</sup> and in diet-induced hepatic steatosis in mice<sup>(31)</sup>; however, its precise contribution to hepatic lipid metabolism remains to be fully elucidated. Although rapamycin treatment has been shown to reduce lipid hepatic synthesis,<sup>(28)</sup> it also impairs lipid storage and catabolism in adipose tissue.<sup>(28)</sup> Thus, lipid imbalance caused by mTORC1 inhibition is more likely to be due to defective lipid degradation rather than increased synthesis. Our experiments aimed to elucidate the molecular mechanism by which mTORC1 is relevant to lipid metabolism and to clarify the different components involved in it, using complementary approaches: *in vitro*, *in vivo*, and *ex vivo*.

Several studies have shown the connection between mTORC1 and peroxisome proliferator-activated receptor gamma with respect to stimulation of lipid uptake and adipogenesis by fat cells,<sup>(32)</sup> which may explain some of the deleterious effects of mTORC1 inhibitors. Recently, it has been reported that cold exposure activates mTORC1 in brown fat tissue and that its inhibition with rapamycin blocks the thermogenic program,<sup>(33)</sup> these observations suggesting an important role for mTORC1 in lipid degradation. However, by increasing autophagy activity, rapamycin treatment may be playing beneficial role in hepatic lipid homeostasis.<sup>(34)</sup> Our experiments dissect how mTORC1 inhibition does not result in increased autophagic degradation of LDs. On the contrary, rapamycin impairs autophagic degradation of lipids. Lipophagy plays an important role in fat utilization, oxygen consumption and energy production.<sup>(6)</sup> Suppression of mTORC1 by rapamycin also significantly reduced ATP generation through fatty acid oxidation. Therefore, the mTORC1 function identified in our study may help to explain clinical observations of hyperlipidemia in response to mTORC1 inhibitors.

HFD-induced steatosis is a commonly used *in vivo* model for inducing NAFLD in mice and which requires at least 3 months of HFD feeding to develop features of the disease.<sup>(35)</sup> In order to favor LD accumulation before the onset of fatty liver and/or steatohepatitis, and to explore the relevance of mTORC1 for the development of fatty liver disease, we fed our mice for one month only. Over this shorter period, HFD activated NF- $\kappa$ B which was associated with a modest stimulation of IL-6 expression. However, HFD in combination with rapamycin treatment resulted in several inflammatory effectors being highly up-regulated. Decreased Abca1 expression in rapamycin treated animals established a connection between lipid handling and inflammation.<sup>(36)</sup> Unresolved inflammation leads to fibrosis<sup>(37)</sup> and obesity is also closely related.<sup>(37)</sup> Addition of rapamycin was also able to increase the expression of TIMP1, which is an important profibrogenic molecule that has diagnostic value in distinguishing patients with fibrosis when they already have NAFLD.<sup>(26)</sup>

Human PCLS are becoming an indispensable tool in liver research and drug development bridging over the animal-human translational gap.<sup>(15,38)</sup> Using this approach, we replicated the main conclusions that were obtained in monolayer *in vitro* experiments and with *in vivo* mouse experiments. Noticeably, rapamycin increased lipid accumulation in the PCLS, which has been also reported in livers from transplants when rapamycin was used as an immunosuppressant.<sup>(39)</sup> Hence, the pharmacological inhibition of mTORC1 can impact on quality of life of patients who have undergone transplant, with a higher risk from NAFLD and cardiovascular diseases.<sup>(29,39)</sup> Further studies will be necessary to show the specific contribution of the Plin3-mTORC1 axis that we have described here in this clinically relevant scenario.

Plin3 is important for LD maturation<sup>(40)</sup> and has been suggested as a biomarker for the early stages of NAFLD.<sup>(4)</sup> We report here that Plin3 is a crucial regulator of lipophagy (Fig. 8). Specifically, Plin3 is required for the recruitment of protein components of the autophagy machinery and for their assembly within the LD in response to lipid loading. Protein sequence suggests that Plin3 might not contain a putative LC3 interacting region (LIR) to mediate its direct binding to LC3,<sup>(41)</sup> but other noncanonical autophagy receptors lacking LIR have recently been described. For example, cell-cycle progression



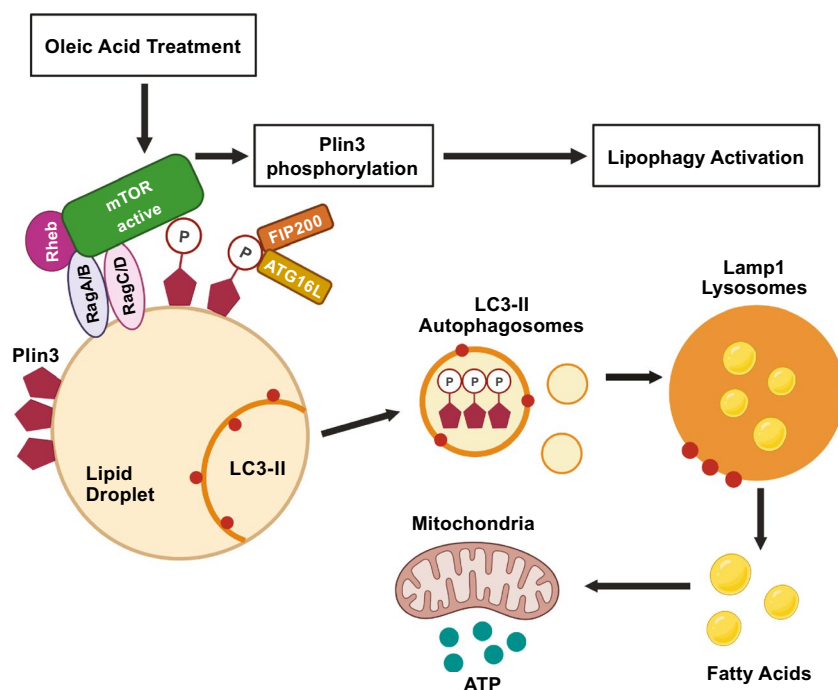


**FIG. 8.** Proposed model where phosphorylated Plin3 acts as a docking protein for lipophagy machinery. OA treatment activates mTORC1 activity to either directly or indirectly phosphorylate Plin3 at LDs. Phosphorylated Plin3 binds the autophagosome formation machinery (FIP200 and ATG16L) to induce lipophagy. The autophagic machinery mobilizes LDs to lysosomes, which generate fatty acids used for energy production by the mitochondria.

gene 1 binds to FIP200 instead of LC3 to promote endoplasmic reticulum autophagy in the pancreas.<sup>(42)</sup> Similarly, our Plin3 pull-downs revealed its strong association with autophagy initiator proteins. Fip200 is a crucial player in the initiation of autophagy and, together with Atg16L1, may also be involved in later stages of autophagosome formation.<sup>(43)</sup> Interaction of FIP200 with Beclin1 was also affected by Plin3 silencing, further supporting its importance for autophagic degradation of LDs.<sup>(44)</sup> We also report that Plin3 regulates the assembly of autophagic complexes on LD, which is dependent on mTORC1. *In silico* analysis supports mTOR as a candidate kinase for Plin3 phosphorylation (<http://www.phosphonet.ca/>), as does our own data showing that treatment with rapamycin inhibits Plin3 phosphorylation, although it remains to be established whether Plin3 is a direct target for mTOR kinase. Besides, Plin3 and mTORC1 are also found interacting on the LD surface. Of note, mTOR is hyperactivated during overfeeding.<sup>(23)</sup> Moreover, phosphorylated mTOR is found in LDs, together with the key proteins required for mTORC1

activation. Therefore, the mTORC1 pathway is active on LDs and through its regulation of Plin3 phosphorylation defines a cellular function for mTORC1 in lipid metabolism and energy production.

In summary, the functional link we have established between Plin3 and mTOR in lipophagy (Fig. 8) and its inhibition by rapamycin reveals a mechanism through which the mTOR axis regulates LD metabolism to suppress the inflammatory and fibrogenic features of NASH. Our demonstration that the mTORC1-Plin3 pathway is active in human PCLS and is required for lipophagy offers an exciting *ex vivo* model to further interrogate the role of mTORC1-Plin3 in hepatosteatosis and to determine its potential as a target for the prevention of NAFLD and other lipid-related pathologies.

*Acknowledgment:* We are members of the Women in Autophagy (WIA), Sociedad Española de Bioquímica y Biología Molecular (SEBBM), Sociedad Española de Autofagia (SEFAGIA), and Instituto de Neurociencia del Principado de Asturias network.

**Author Contributions:** M.G.-M. performed experiments and analyzed the data. A.S.-L., J.L., H.L.P., A.L.C., R.S.S., A.W., S.W., J.F., J.H., and R.A.B. assisted with the experiments or contributed materials. L.A.B., J.M., J.P.B., and F.O. provided intellectual input. M.G.-M. conceived the idea, designed the experiments, interpreted data, and wrote the manuscript. A.S.-L. helped to write the manuscript. J.P.B., V.I.K., F.O., and D.A.M. supervised the project and edited the manuscript. All authors commented on and reviewed the manuscript.

## REFERENCES

- Anstee QM, Reeves HL, Kotsiliti E, Govaere O, Heikenwalder M. From NASH to HCC: current concepts and future challenges. *Nat Rev Gastroenterol Hepatol* 2019;16:411-428.
- Gluchowski NL, Becuwe M, Walther TC, Farese RV Jr. Lipid droplets and liver disease: from basic biology to clinical implications. *Nat Rev Gastroenterol Hepatol* 2017;14:343-355.
- Kaushik S, Cuervo AM. Degradation of lipid droplet-associated proteins by chaperone-mediated autophagy facilitates lipolysis. *Nat Cell Biol* 2015;17:759-770.
- Pawella LM, Hashani M, Eiteneuer E, Renner M, Bartenschlager R, Schirmacher P, et al. Perilipin discerns chronic from acute hepatocellular steatosis. *J Hepatol* 2014;60:633-642.
- Niso-Santano M, Malik SA, Pietrocola F, Bravo-San Pedro JM, Mariño G, Cianfanelli V, et al. Unsaturated fatty acids induce non-canonical autophagy. *EMBO J* 2015;34:1025-1041.
- Singh R, Kaushik S, Wang Y, Xiang Y, Novak I, Komatsu M, et al. Autophagy regulates lipid metabolism. *Nature* 2009;458:1131-1135.
- Singh R, Xiang Y, Wang Y, Baikati K, Cuervo AM, Luu YK, et al. Autophagy regulates adipose mass and differentiation in mice. *J Clin Invest* 2009;119:3329-3339.
- Kaushik S, Cuervo AM. AMPK-dependent phosphorylation of lipid droplet protein PLIN2 triggers its degradation by CMA. *Autophagy* 2016;12:432-438.
- Gatica D, Lahiri V, Klionsky DJ. Cargo recognition and degradation by selective autophagy. *Nat Cell Biol* 2018;20:233-242.
- Schroeder B, Schulze RJ, Weller SG, Sletten AC, Casey CA, McNiven MA. The small GTPase Rab7 as a central regulator of hepatocellular lipophagy. *HEPATOLOGY* 2015;61:1896-1907.
- Rabanal-Ruiz Y, Korolchuk VI. mTORC1 and nutrient homeostasis: the central role of the lysosome. *Int J Mol Sci* 2018;19:818.
- Mensah LB, Goberdhan DCI, Wilson C. mTORC1 signalling mediates PI3K-dependent large lipid droplet accumulation in *Drosophila* ovarian nurse cells. *Biol Open* 2017;6:563-570.
- Brasaemle DL, Wolins NE. Isolation of lipid droplets from cells by density gradient centrifugation. *Curr Protoc Cell Biol* 2006;72:3.15.1-3.15.13.
- Martinez-Lopez N, Garcia-Macia M, Sahu S, Athonvarangkul D, Liebling E, Merlo P, et al. Autophagy in the CNS and periphery coordinate lipophagy and lipolysis in the brown adipose tissue and liver. *Cell Metab* 2016;23:113-127.
- Paish HL, Reed LH, Brown H, Bryan MC, Govaere O, Leslie J, et al. A bioreactor technology for modeling fibrosis in human and rodent precision-cut liver slices. *HEPATOLOGY* 2019;70:1377-1391.
- Alkhatatbeh MJ, Lincz LF, Thorne RF. Low simvastatin concentrations reduce oleic acid-induced steatosis in HepG2 cells: an in vitro model of non-alcoholic fatty liver disease. *Exp Ther Med* 2016;11:1487-1492.
- Liu Y, Liao L, Chen Y, Han F. Effects of daphnetin on lipid metabolism, insulin resistance and oxidative stress in OA-treated HepG2 cells. *Mol Med Rep* 2019;19:4673-4684.
- Rohwedder A, Zhang Q, Rudge SA, Wakelam MJ. Lipid droplet formation in response to oleic acid in Huh-7 cells is mediated by the fatty acid receptor FFAR4. *J Cell Sci* 2014;127:3104-3115.
- Lagrutta LC, Montero-Villegas S, Layerenza JP, Sisti MS, Garcia de Bravo MM, Ves-Losada A. Reversible nuclear-lipid-droplet morphology induced by oleic acid: a link to cellular-lipid metabolism. *PLOS ONE* 2017;12:e0170608.
- Klionsky DJ, Abdelmohsen K, Abe A, Abedin MJ, Abeliovich H, Acevedo Arozena A, et al. Guidelines for the use and interpretation of assays for monitoring autophagy (3rd edition). *Autophagy* 2016;12:1-222.
- Ktistakis NT, Tooze SA. Digesting the expanding mechanisms of autophagy. *Trends Cell Biol* 2016;26:624-635.
- Babashamsi MM, Koukhaloo SZ, Halalkhor S, Salimi A, Babashamsi M. ABCA1 and metabolic syndrome; a review of the ABCA1 role in HDL-VLDL production, insulin-glucose homeostasis, inflammation and obesity. *Diabetes Metab Syndr* 2019;13:1529-1534.
- Zoncu R, Efeyan A, Sabatini DM. mTOR: from growth signal integration to cancer, diabetes and ageing. *Nat Rev Mol Cell Biol* 2011;12:21-35.
- Sancak Y, Bar-Peled L, Zoncu R, Markhard AL, Nada S, Sabatini DM. Ragulator-Rag complex targets mTORC1 to the lysosomal surface and is necessary for its activation by amino acids. *Cell* 2010;141:290-303.
- Moran-Salvador E, Garcia-Macia M, Sivaharan A, Sabater L, Zaki MYW, Oakley F, et al. Fibrogenic activity of MECP2 is regulated by phosphorylation in hepatic stellate cells. *Gastroenterology* 2019;157:1398-1412.e9.
- Yilmaz Y, Eren F. Serum biomarkers of fibrosis and extracellular matrix remodeling in patients with nonalcoholic fatty liver disease: association with liver histology. *Eur J Gastroenterol Hepatol* 2019;31:43-46.
- Paish HL, Reed LH, Brown H, Bryan MC, Govaere O, Leslie J, et al. A bioreactor technology for modelling fibrosis in human and rodent precision-cut liver slices. *HEPATOLOGY* 2019;70:1377-1391.
- Houde VP, Brule S, Festuccia WT, Blanchard PG, Bellmann K, Deshaies Y, et al. Chronic rapamycin treatment causes glucose intolerance and hyperlipidemia by upregulating hepatic gluconeogenesis and impairing lipid deposition in adipose tissue. *Diabetes* 2010;59:1338-1348.
- Gitto S, Villa E. Non-alcoholic fatty liver disease and metabolic syndrome after liver transplant. *Int J Mol Sci* 2016;17:490.
- Han C, Wei S, He F, Liu D, Wan H, Liu H, et al. The regulation of lipid deposition by insulin in goose liver cells is mediated by the PI3K-AKT-mTOR signaling pathway. *PLoS One* 2015;10:e0098759.
- Kim K, Qiang L, Hayden MS, Sparling DP, Purcell NH, Pajvani UB. mTORC1-independent Raptor prevents hepatic steatosis by stabilizing PHLPP2. *Nat Commun* 2016;7:10255.
- Festuccia WT, Blanchard PG, Belchior T, Chimin P, Paschoal VA, Magdalon J, et al. PPAR $\gamma$  activation attenuates glucose intolerance induced by mTOR inhibition with rapamycin in rats. *Am J Physiol Endocrinol Metab* 2014;306:E1046-E1054.
- Labbe SM, Mouchiroud M, Caron A, Secco B, Freinkman E, Lamoureux G, et al. mTORC1 is required for brown adipose tissue recruitment and metabolic adaptation to cold. *Sci Rep* 2016;6:37223.
- Lin CW, Zhang H, Li M, Xiong X, Chen XI, Chen X, et al. Pharmacological promotion of autophagy alleviates steatosis and

- injury in alcoholic and non-alcoholic fatty liver conditions in mice. *J Hepatol* 2013;58:993-999.
- 35) Velázquez KT, Enos RT, Bader JE, Sougiannis AT, Carson MS, Chatzistamou I, et al. Prolonged high-fat-diet feeding promotes non-alcoholic fatty liver disease and alters gut microbiota in mice. *World J Hepatol* 2019;11:619-637.
- 36) Liu M, Chung S, Shelness GS, Parks JS. Hepatic ABCA1 and VLDL triglyceride production. *Biochim Biophys Acta* 2012;1821:770-777.
- 37) Marcelin G, Silveira ALM, Martins LB, Ferreira AV, Clément K. Deciphering the cellular interplays underlying obesity-induced adipose tissue fibrosis. *J Clin Invest* 2019;129:4032-4040.
- 38) Martin SZ, Wagner DC, Hörner N, Horst D, Lang H, Tagscherer KE, et al. Ex vivo tissue slice culture system to measure drug-response rates of hepatic metastatic colorectal cancer. *BMC Cancer* 2019;19:1030.
- 39) Neff GW, Montalbano M, Tzakis AG. Ten years of sirolimus therapy in orthotopic liver transplant recipients. *Transplant Proc* 2003;35:209S-216S.
- 40) Bulankina AV, Deggerich A, Wenzel D, Mutenda K, Wittmann JG, Rudolph MG, et al. TIP47 functions in the biogenesis of lipid droplets. *J Cell Biol* 2009;185:641-655.
- 41) Jacomin AC, Samavedam S, Promponas V, Nezis IP. iLIR database: A web resource for LIR motif-containing proteins in eukaryotes. *Autophagy* 2016;12:1945-1953.
- 42) Smith MD, Harley ME, Kemp AJ, Wills J, Lee M, Arends M, et al. CCPG1 is a non-canonical autophagy cargo receptor essential for ER-phagy and pancreatic ER proteostasis. *Dev Cell* 2018;44:217-232.e11.
- 43) Nishimura T, Kaizuka T, Cadwell K, Sahani MH, Saitoh T, Akira S, et al. FIP200 regulates targeting of Atg16L1 to the isolation membrane. *EMBO Rep* 2013;14:284-291.
- 44) Hara T, Takamura A, Kishi C, Iemura S, Natsume T, Guan JL, et al. FIP200, a ULK-interacting protein, is required for autophagosome formation in mammalian cells. *J Cell Biol* 2008;181:497-510.

Author names in bold designate shared co-first authorship.

## Supporting Information

Additional Supporting Information may be found at [onlinelibrary.wiley.com/doi/10.1002/hep.32048/suppinfo](http://onlinelibrary.wiley.com/doi/10.1002/hep.32048/suppinfo).